The effect of platelet rich plasma and nigella sativa on experimentally induced skeletal muscle injury in adult male albino rats: Histological and immunohistochemical study

ABSTRACT

Background: Injuries involving skeletal muscle disturb millions across the globe. Platelet-rich plasma (PRP) is encouraging strategy for improving tissue healing. Nigella sativa (NS) have broad-spectrum therapeutic properties. **Aim:** The research assesses the potential beneficial impact of PRP and NS on muscle injury. **Materials and Methods:** 112 animals were allocated into five experimental groups: Group I, The control group. Group II: administered only glycerol. Group III: administered glycerol then PRP intramuscularly. Group IV: administered NS orally for 21days then glycerol. Group V: given NS orally for 21days then glycerol then PRP. Half of the rats were euthanized 7 days after glycerol injection (subgroups a) and the other half 14 days after injection (subgroups b). H&E, Masson's trichrome staining, myogenin immunostaining, and ultrastructural analysis were performed on muscle sections. **Results:** Group II exhibited destruction of myofibers and significant ($P<0.01$) fibrosis.Group III demonstrated moderate amelioration with significant ($P<0.01$) decline in fibrosis and significant ($P<0.01$) upregulation in myogenin reaction. Group IV showed mild improvement, with significant ($P<0.01$) decline in fibrosis and limited regeneration. Group V exhibited the most pronounced amelioration, with very significant ($P<0.01$) decrease in fibrosis and extensive significant ($P<0.01$) upregulation in myogenin reaction. **Conclusion:** Administration of PRP and NS reduced damage and promoted myoregeneration and differentiation with PRP giving more improvement. The combined administration of PRP and NS markedly attenuated damage and enhanced myoregeneration and differentiation.

Key Words: Skeletal muscle injuries, glycerol, platelet rich plasma, nigella sativa, myogenin.

INTRODUCTION

Skeletal muscle injuries are widely occurring events. Skeletal muscles are essential for regulating energy and protein metabolism, in addition to their role in generating force for locomotion and maintaining stability. Muscle injuries arising from contusions, strains, lacerations, burns, ischemia, toxins, chemical agents, or vigorous exercise can compromise these fundamental functions [1].

As suboptimal muscle repair can result in persistent functional impairments, many studies has been dedicated to developing approaches to enhance the regenerative process. Glycerol (50%) administered intramuscularly elicits degenerative changes resembling the degenerative changes in Duchene muscular dystrophies and may serve as an appropriate experimental approach for investigating skeletal muscle damage and repair [2].

Muscle damage activates progressive but intersecting phases—degeneration, inflammation, repair, and fibrosis—driven by complex molecular and cellular interactions. [3].

Satellite cells (SCs) play a central role in skeletal muscle regeneration. Under homeostatic state, SCs stay dormant. As a result of injury or exposure to growth factors, SCs rapidly reenter the cell cycle. Once activated, SCs migrate and undergo extensive proliferation to facilitate muscle regeneration. The regeneration capacity of SCs is compromised by aging, severe muscle loss and genetic myopathy [4, 5].

Regenerative medicine represents one of the most rapidly advancing fields within both human and veterinary restorative therapies, particularly in orthopedics and neurology. PRP constitutes one of the most rapidly emerging regenerative techniques. PRP promotes the accelerated repair of injured tissues [6].

The primary growth factors contained within platelets comprise insulin-like growth factor (IGF), platelet-derived growth factor (PDGF), vascular endothelial growth factor (VEGF), transforming growth factor (TGFβ) and epidermal growth factor (EGF). The tissue regeneration phase relies on these growth factors and encompasses intricate, overlapping processes typically classified as hemostasis, inflammation, proliferation, and remodeling [7, 8].

Growth factors released from platelets are essential proteins which can support and maintain cell growth and survival. These growth factors influence both differentiated and undifferentiated cells in healing process. They induce tissue regeneration by reducing apoptosis, exerting anti-inflammatory action, and promoting angiogenesis and cell proliferation through paracrine and autocrine signaling mechanisms [6, 9].

Nigella sativa (NS) is regarded as a significant herbal remedy. Prophet Muhammad (Peace Be Upon Him) referred to it as a cure for every illness except death [10] . NS are extensively recognized for exhibiting a broad spectrum of pharmacological activities, predominantly ascribed to their antioxidative, anti-inflammatory, antineoplastic, antimicrobial, nephroprotective, and neuroprotective effects [11, 12]

This work was intended to explore the impacts of PRP and NS on skeletal muscle injury triggered by glycerol administration induced by glycerol.

MATERIALS AND METHODS

The study was done in the Animal House Unit of the Faculty of Veterinary Medicine, Benha University, from June 2022 to mid-July 2022. This study utilized 112 adult male albino rats, each weighing between 150 and 200 grams. Rigorous hygiene and husbandry practices were implemented to maintain the animals in optimal health; Rats were kept in standard laboratory cages, kept in regulated environmental factors and provided with standard chow and free access of water. The measures involving animal handling were adhered to institutional ethical standards and were monitored by the animal facility staff. The consent code received from the research ethics committee was MD 15-1-2022.

Drugs used:

a) Glycerol was obtained from El Gomhouria pharmaceuticals company. Its batch No. was D210909-13-1. A single intramuscular injection of 0.5 ml/kg of 50% glycerol prepared in normal saline was administered into the back of the right leg [13].

b) Platelet rich plasma (PRP) was processed under standardized conditions in the Central Lab of Faculty of Veterinary Medicine, Benha University. It was administered as a single dose of 1ml /kg intramuscularly in the back of the right leg [14].

c) Nigella sativa seeds (NS) were obtained from local herbal market. The seeds were grinded by electric grinder before usage to form powder. The powder was given orally by gastric tube, dissolved in distilled water. Each rat received 2g/kg nigella sativa orally dissolved in 4ml distilled water each day for 21 days [15, 16].

Experimental design:

Rats were assigned to five experimental groups as outlined below;

1. **Group I :** comprised 56 animals, further distributed among four subgroups:

Subgroup I-1 (14 rats): animals received nothing.

Subgroup I-2 (14 rats): animals were injected intramuscularly with 0.5ml of saline (solvent of glycerol) at the time of glycerol injection.

Subgroup I-3 (14 rats): animals were injected with 1 ml\kg plasma (media of platelets) intramuscularly in the back of the right leg at the time of platelet rich plasma injection.

Subgroup I-4 (14 rats): Animals received 4ml distilled water /kg by gastric tube (solvent of nigella sativa) daily for 21 days.

The rats from each subgroup were equally divided into 2 subgroups; a (n=7) and b (n=7).

2. Group II (Muscle injury group): It contained 14 rats, which were given a single dose of 0.5 ml of 50% glycerol /kg intramuscularly in the back of the right leg. Animals were assigned into 2 subgroups; IIa (n=7) and IIb (n=7).

3. Group III (PRP group): It contained 14 rats. Each rat was injected with glycerol as group II, then with 1 ml\kg PRP intramuscularly in the back of the right leg one hour after glycerol injection. Rats were equally assigned into 2 subgroups; IIIa (n=7) and IIIb (n=7).

4. **Group IV (NS group):** It contained 14 rats. Each rat received NS orally by gastric tube, NS was dissolved in 4ml distilled water every day for 21 days and then was injected with glycerol as group II one hour after the last dose of NS in the 21st day. Rats were equally assigned into 2 subgroups; IVa (n=7) and IV =b (n=7).

5. **Group V (PRP+NS group):** It contained 14 rats. Animals received NS as group IV, then glycerol as group II and then PRP as group III. Rats were equally assigned into 2 subgroups; Va (n=7) and Vb (n=7).

Half of rats from all groups were euthanized 7 days after glycerol administration (subgroup a) and the other half 14 days after glycerol administration (subgroup b).

Preparation of platelet rich plasma:

About 3 mL of blood from each rat was taken from the retro-orbital venous plexus. Blood specimens were conveyed into sterile tubes containing sodium citrate as an anticoagulant. The samples underwent a two-step centrifugation process. An initial centrifugation for 10 minutes at 1600 rpm yielded three distinct layers: the bottom one, comprising erythrocytes, the intermediate layer consisting of a buffy coat enriched in leukocytes, and the top layer containing plasma. The plasma supernatant was carefully aspirated and then centrifuged at 2000 rpm for 10 minutes, leading to the formation of two distinct compartments. The platelets were sedimented at the bottom of the tubes. The upper portion of superior compartment had been discarded. The lower part of the superior compartment was retained in the tube together with the inferior compartment to produce the platelet rich plasma [17, 18].

Collection and preparation of tissue samples for light microscopic study:

Following a fasting period, the rats were anesthetized using ether and euthanized via cervical dislocation. Subsequently, dissection was performed, and tissue samples from the right gastrocnemius muscle were excised from all experimental groups at specific time points (7 and 14 days following glycerol administration). The tissue sections were divided into 3 parts for H&E, Masson's trichrome stainimg and myogenin immunostaining. The samples underwent fixation in 10% formol saline. The tissues were subsequently processed for histological examination [19, 20].

Immunohistochemical study

Immunohistochemical staining was performed utilizing labeled streptavidin–biotin technique. Anti-myogenin (primary antibody), was a mouse monoclonal antibody (Clone MyG007, also known as F5D), provided by Dako (UniProt ID: P20428 MYOG-

R). A universal detection system employing a biotinylated secondary antibody was utilized. The counterstain applied was Mayer's hematoxylin. Human rhabdomyosarcoma tissue served as the positive control, exhibiting a characteristic brown nuclear staining pattern for myogenin. To exclude nonspecific immunostaining, negative controls were implemented through the exclusion of anti-myogenin antibody [20].

Electron microscopic analysis

Muscle specimens were initially placed in glutaraldehyde (2.5%), followed by postfixation in osmium tetroxide (1%). Samples were processed at the Electron Microscopy Unit, Faculty of Medicine, Tanta University. Semi-thin (0.5–1 μm) sections obtained. Subsequently, tissue ultrathin sections (50–70 nm) were contrasted utilizing uranyl acetate and lead citrate. Examination was performed by a JEOL transmission electron microscope (JEM-100 SX; JEOL, Tokyo, Japan) at the same facility [21].

Morphometric study

Collagen mean area percentage and myogenin-positive nuclear immunoreaction was quantitatively assessed from seven images from seven non-intersecting fields of each group and subgroup of rats, analyzed with Image-Pro Plus program version 6.0 (Media Cybernetics Inc., Bethesda, Maryland, USA).

Statistical analysis

Data were analyzed using IBM SPSS Statistics 22.0 (IBM Corp., Armonk, NY, USA). Group comparisons were conducted with one-way ANOVA with subsequent LSD post hoc testing. Results are presented as mean ± SD, with $p < 0.01$ considered significant as provided in **Tables (1)** and **(2)**.

RESULTS

***Hematoxylin and Eosin stain results**:*

1- Group I (Control group):

Sections of gastrocnemius muscle of all subgroups revealed the normal histological architecture. In longitudinal section, myofibers The myofibers were long, cylindrical, and aligned in parallel with multiple peripherally located flat nuclei under the sarcolemma. The sarcoplasm appeared acidophilic with transverse striations. In transverse section, the muscle was consisted of bundles of myofibers. Individual fibers appeared polygonal with peripherally located nuclei as in **(Figs. 1a & 1b).**

2- Group II (Muscle injury group):

Subgroup IIa: showed destruction of skeletal muscle fibers. Sarcoplasm showed vacuolations. There was inflammatory infiltrate among the muscle fibers. The intervening spaces between muscle fibers were widened. There were some regenerating fibers with internalization of myonuclei **(Figs. 1c & 1d)**.

Subgroup IIb: loss of parts of the fibers and vacuolations of sarcoplasm with widened spaces between the fibers were still present. Inflammatory cellular infiltrate was still present. Internalization of myonuclei was still present indicating that trials for regeneration were still occurring and was not completed **(Figs. 1e &1f)**.

3- Group III (PRP group):

Subgroup IIIa: There were regenerating myofibers with internalized myonuclei and some vacuolations of muscle fibers. There were normal myofibers with peripheral flat nuclei and the extra cellular spaces showed apparently little widening **(Figs. 1g & 1h).**

Subgroup IIIb: Some fibers exhibited normal morphology with transverse striations and flat peripheral nuclei but some others showed little vacuolations and internalized nuclei in regenerating fibers as in **(Figs. 1i & 1j).**

4- Group IV (NS group):

Subgroup IVa: There were some splitting in muscle fibers with some widening of spaces between the fibers and there were some regenerating muscle fibers with internalization of myonuclei **(Figs. 1k & 1l).**

Subgroup IVb: There were normal muscle fibers with peripheral flat nuclei and the extra cellular spaces showed little widening. There were some little vacuolations in muscle fibers with some regenerating muscle fibers with internalized myonuclei **(Figs. 1m & 1n).**

5- Group V (NS + PRP group):

Subgroup Va: Most of the myofibers revealed normal structure. There was apparently little splitting of the myofibers with little widening of the extra cellular spaces. There were regenerating muscle fibers with internalization of myonuclei **(Figs. 1o & 1p).**

Subgroup Vb: The muscle fibers were apparently like normal with transverse striations and flat peripheral nuclei **(Figs. 1q & 1r).**

Masson's Trichrome results*:*

1- **Group I (Control group):** all control subgroups exhibited minimal presence of collagen fibers within the connective tissue separating the myofibers **(Fig. 2a).**
2- **Group II (muscle injury group):** An evident increase in collagen fibers deposition within the connective tissue separating muscle fibers was observed in both Subgroups IIa and IIb, as shown in **(Fig. 2b)** and **(Fig. 2c)**, respectively.
3- **Group III (PRP group):** Subgroups IIIa and IIIb exhibited a slight deposition of collagen fibers within the connective tissue between muscle fibers, as shown in **(Fig. 2d)** and **(Fig. 2e)**, respectively.
4- **Group IV (NS group):** Subgroup IVa showed a moderate deposition of collagen fibers within the connective tissue between muscle fibers, as seen in **(Fig. 2f)**, while Subgroup IVb exhibited a slight deposition, as shown in **(Fig. 2g).**
5- **Group V (NS+PRP group):** Subgroup Va showed minimal deposition of collagen between the myofibers, as seen in **(Fig. 2h)**. Similarly, Subgroup Vb exhibited a

very minimal amount of collagen within the connective tissue separating the apparently normal muscle fibers **(Fig. 2i).**

Results of immunohistochemical staining for myogenin:

Positive reaction showed brown immunopositive nuclei at the sarcolemma and between the muscle fibers.

1- **Group I (Control group):** All control subgroups demonstrated very minimal myogenin immunoreaction **(Fig. 3a).**
2- **Group II (muscle injury group):** Subgroups IIa and IIb demonstrated low myogenin immunoreactivity, reflected by a low area percentage of positive staining as seen in **Fig. 3b** and **Fig. 3c,** respectively**.**
3- **Group III (PRP group):** Subgroups IIIa and IIIb demonstrated a moderate level of myogenin immunoreactivity, as exhibited in **Fig. 3d** and **Fig. 3e**, respectively."
4- **Group IV (NS group):** Subgroups IVa and IVb demonstrated weak myogenin immunoreactivity, as seen in **Fig. 3f** and **Fig. 3g**, respectively.
5- **Group V (NS + PRP group):** Subgroups Va and Vb demonstrated strong myogenin immunoreactivity, with a high area percentage of positively stained regions evident in **Fig. 3h** and **Fig. 3i,** respectively.

Morphometric and statistical analysis:

The mean percentage area for collagen, assessed, and for myogenin immunoreactivity are provided in **Tables (1)** and **(2)**, respectively, and exhibited in **Fig. 2j** and **Fig. 3j**, respectively. No notable variations ($P < 0.01$) were identified between subgroups IIa and IIb in either collagen deposition or myogenin immunostaining. However, relative to group I, both subgroups IIa and IIb exhibited a significant elevation ($P < 0.01$) in collagen fibers accumulation and myogenin immunoreactivity.

Relative to group II, a significant reduction ($P < 0.01$) in collagen deposition was noted in groups III, IV, and V. In comparison to group I, subgroup Va demonstrated a statistically significant upregulation ($P < 0.01$) in collagen accumulation, whereas the increase detected in subgroup Vb was insignificant ($P < 0.01$). Regarding myogenin immune reaction, groups II, III, IV, and V, all exhibited a significant increase ($P < 0.01$) when compared to Group I. Relative to group II, both groups III and V exhibited a

further significant increase ($P < 0.01$), while group IV exhibited a significant decline ($P < 0.01$) in myogenin immunoreactivity.

Ultrastructural results:

1- Group I (Control group):

Ultrathin sections analysis of all control subgroups demonstrated normal morphological features. The myofibers were predominantly composed of myofibrils, which consisted of regularly arranged myofilaments responsible for the characteristic striated pattern. These striations were formed by alternating light (I) and dark (A) bands aligned in register across the fibers. Each A band contained a paler H zone at its center. The H zone contained a central dark M line. While, each I band was intersected by a dense Z line. Sarcomeres were regularly arranged between consecutive Z lines. Peripheral oval nuclei with prominent nucleoli were observed. Mitochondria were small and primarily located near the Z lines, interspersed between myofibrils and adjacent to the nuclei (**Figs. 4a & 4b).**

2- Group II (muscle injury group):

Subgroup IIa exhibited pronounced skeletal muscle damage and necrosis characterized by disruption, fragmentation, degeneration, thinning, and disorganization of myofibrils. These alterations were accompanied by widened intermyofibrillar spaces and focal areas of complete cytoplasmic loss. The sarcolemma appeared irregular and undulated, indicative of muscle fiber atrophy. Additionally, some nuclei were shrunken with irregular contours. Mitochondria demonstrated structural abnormalities, including altered matrix density. Furthermore, collagen fiber deposits were evident within the endomysium **(Fig. 4c).** Subgroup IIb demonstrated persistence of several ultrastructural alterations observed in Subgroup IIa **(Fig. 4d).**

3- Group III (PRP group):

Subgroup IIIa exhibited regions with preserved ultrastructure, characterized by clearly defined alternating dark and light bands and normal nuclei. However, focal areas displayed signs of injury, including cytoplasmic vacuolations. Mitochondrial

morphology was variable, with some mitochondria appearing small and spherical, while others were elongated and dilated **(Fig. 5a).**

Subgroup IIIb showed that most of the areas exhibited normal structure and only little injury persisted as vacuolations in the cytoplasm. There were elongated mitochondria **(Fig. 5b).**

4- Group IV (NS group):

Subgroup IVa showed presence of areas exhibiting normal structure as alternating dark and light bands. Some other areas exhibited mild injury as vacuolations in the cytoplasm and some widening of the spaces between the myofibrils. Some of the mitochondria were normal small spherical and others were elongated **(Fig. 5c).** Subgroup IVb showed that some of the areas exhibited normal structure and only some injury persisted as vacuolations in the cytoplasm. There were some dilated and elongated mitochondria **(Fig. 5d).**

5- Group V (NS + PRP group):

Subgroup Va showed that most of the areas of the sections exhibited normal structure as alternating dark and light bands. Other little areas exhibited very little injury as little degenerated myofibrils. Small spherical mitochondria were present around Z lines and in between the myofibrils. There were some elongated mitochondria as in **(Fig. 5e).** The sections in subgroup Vb were apparently like normal. There were alternating dark and light bands and oval nucleus with prominent nucleolus. Small spherical mitochondria were present along Z lines and inbetween the myofibrils **(Fig. 5f).**

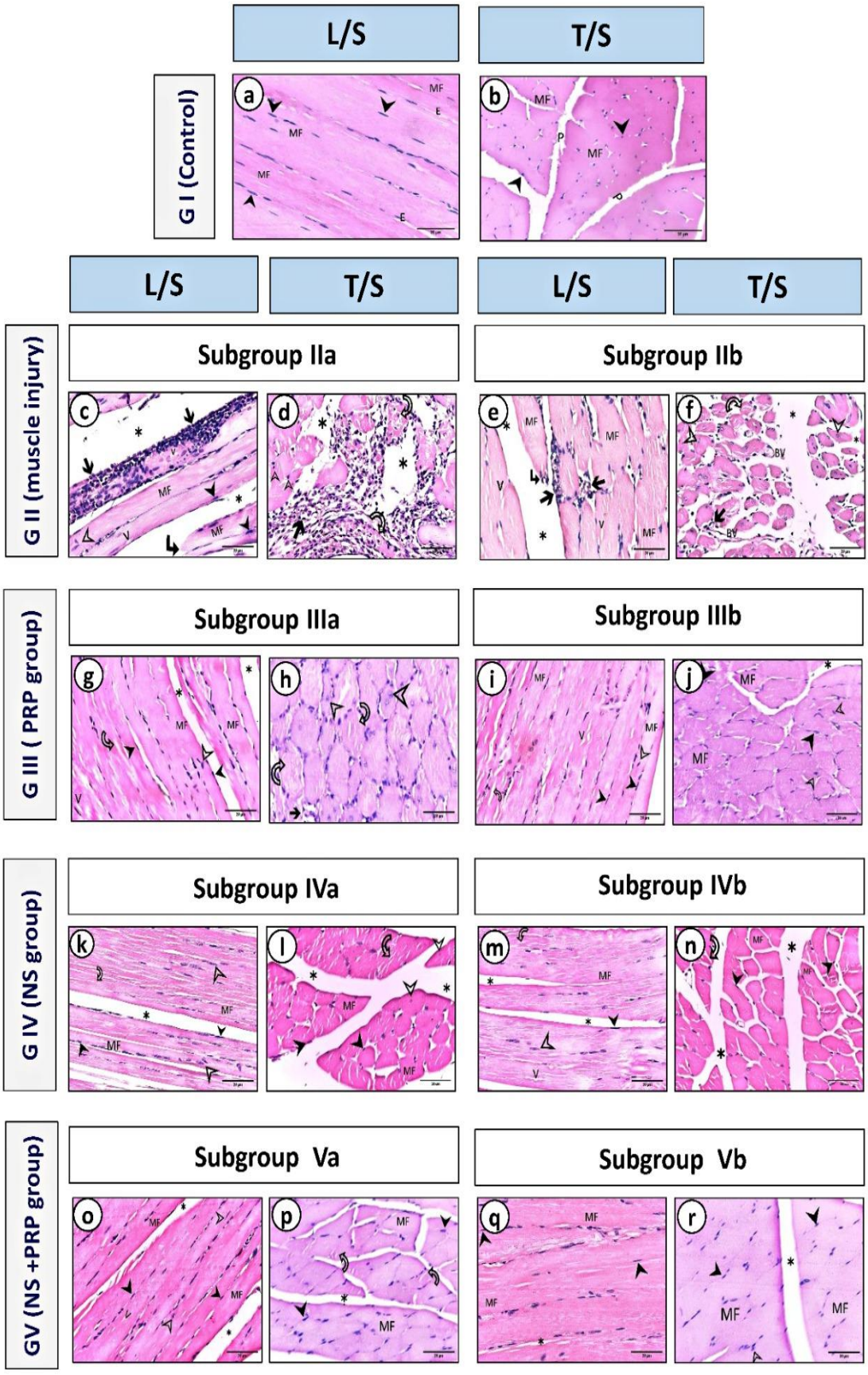
L/S
T/S
G I (Control)
a
b
MF
E
P
L/S
T/S
L/S
T/S
G II (muscle injury)
Subgroup IIa
Subgroup IIb
c
d
e
f
BV
G III (PRP group)
Subgroup IIIa
Subgroup IIIb
g
h
i
j
G IV (NS group)
Subgroup IVa
Subgroup IVb
k
l
m
n
GV (NS +PRP group)
Subgroup Va
Subgroup Vb
o
p
q
r

Fig. 1: Photomicrographs of rat gastrocnemius muscle sections stained by H&E (X 400): [a]: Shows long and parallel skeletal muscle fibers having acidophilic cytoplasm with transverse striations **(MF)** and flat peripheral nuclei **(solid arrow heads)** directly underneath the sarcolemma with little intervening spaces between the muscle fibers denoting the site of endomysium **(E)**. **[b]** Shows bundles of polygonal muscle fibers **(MF)** with little spaces between them and rather uniform in size, peripherally located nuclei **(solid arrow heads**) and perimysium **(P)** enclosing the muscle bundles. **[c] &** [**d]**: Display skeletal muscle fibers **(MF)** with flat peripheral nuclei (**solid arrow heads**), loss and interruption of muscle fibers **(angled arrow)**, degenerated muscle fibers **(curved arrows)**, vacuolations in the sarcoplasm (**V**), abundant inflammatory cellular infiltrate **(straight arrows),** very wide spaces between the muscle fibers (*****) and internalized central myonuclei **(hollow arrow heads)** which are large oval and pale. **[e] & [f]:** Show skeletal muscle fibers **(MF)**, loss and interruption of muscle fibers **(angled arrow),** vacuolations in the sarcoplasm (**V**), degeneration and splitting of the muscle fibers **(curved arrows)**, inflammatory cellular infiltrate **(straight arrows),** very wide spaces between the muscle fibers (*****) with blood vessels **(BV)** and internalized central nuclei in the muscle fibers **(hollow arrow heads). [g] & [h]:** Show skeletal muscle fibers **(MF)** with flat peripheral nuclei (**solid arrow heads**), apparently little degeneration and splitting of myofibers **(curved arrows),** little sarcoplasmic vacuolations (**V**), little widening of spaces between the muscle fibers (*****) and many internalized pale central nuclei in the muscle fibers **(hollow arrow heads)**. **[i] & [j]:** Showing skeletal muscle fibers **(MF)** with flat peripheral nuclei (**solid arrow heads**), little splitting of myofibers **(curved arrow)** with little vacuolations in sarcoplasm (**V**), small spaces between muscle fibers (*****) and internalized central nuclei in the muscle fibers **(hollow arrow heads). [k] & [l]:** Showing skeletal muscle fibers **(MF)** with flat peripheral nuclei (**solid arrow heads)**, some splitting in the muscle fibers **(curved arrow)**, some widening of spaces between the muscle fibers (*****) and internalized central myonuclei **(hollow arrow heads). [m] & [n]** Showing skeletal muscle fibers **(MF)** with flat peripheral nuclei (**solid arrow heads**), some splitting in the muscle fibers **(curved arrows),** little vacuolations in the sarcoplasm (**V**)**,** little widening of the spaces between the muscle fibers (*****) and internalized central myonuclei **(hollow arrow heads)**. **[o] & [p]:** Showing apparently like normal skeletal muscle fibers **(MF)** with flat peripheral nuclei (**solid arrow heads**), very small spaces between the muscle fibers, very little splitting in the muscle fibers **(curved arrows)** and internalized central myonuclei **(hollow arrow heads). [q] & [r]**: Showing almost normal skeletal muscle fibers **(MF)** with flat peripheral nuclei (**solid arrow heads**), minimal intervening spaces between the muscle fibers (*****) similar to normal and internalized central myonucleus **(hollow arrow head).**

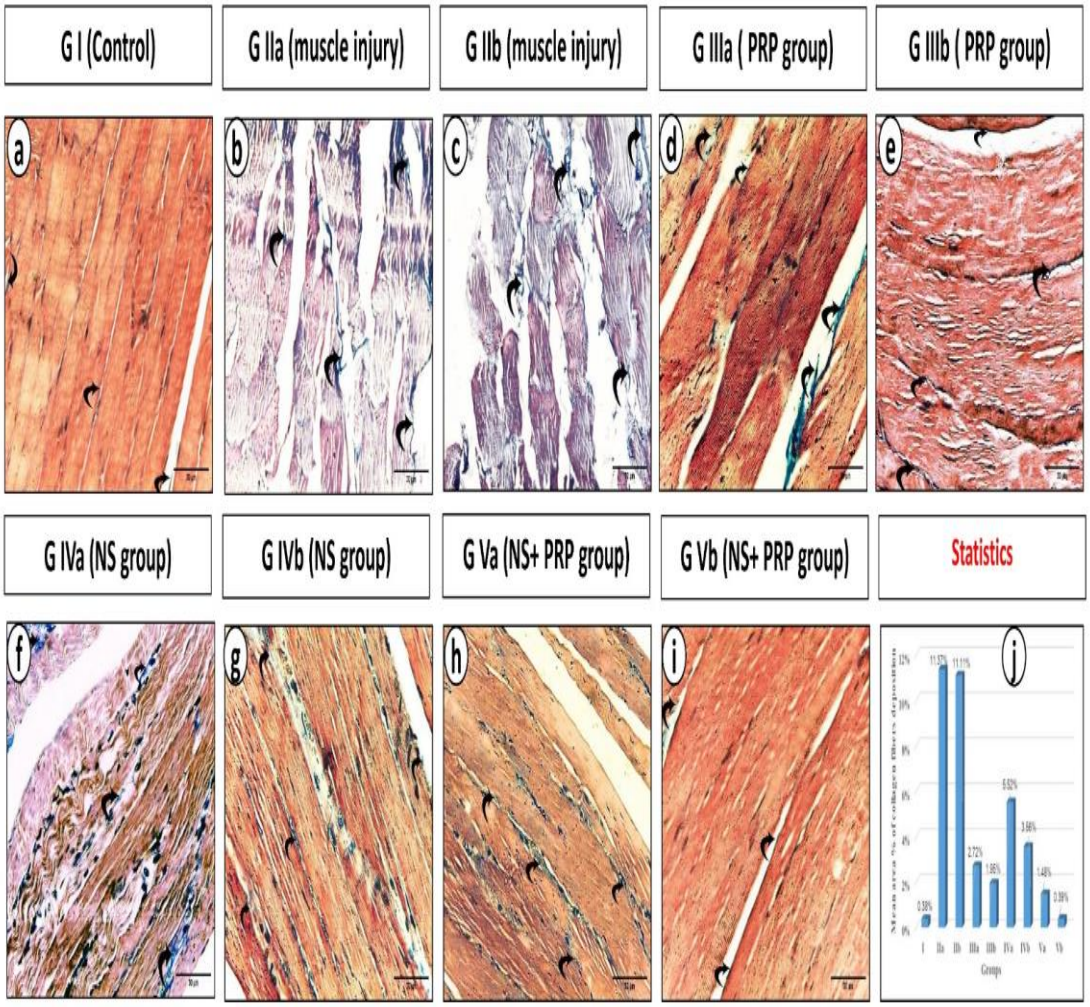

Fig.2: [a –i]: Photomicrographs of rat gastrocnemius muscle sections stained with Masson's trichrome (X400), demonstrating collagen fibers deposition patterns between muscle fibers (arrows) which appear very minimal in control group **[a]**, extreme in subgroup IIa **[b**] and very extreme in subgroup IIb **[c]. [d]:** Slight collagen fibers in subgroup IIIa**. [e]**: Minimal collagen deposition in subgroup IIIb **[f]:** Moderate collagen fibers deposition in subgroup IVa **[g]**: Slight collagen accumulation in subgroup IVb **[h]:** Minimal collagen fibers deposition in subgroup Va. **[i]:** Very minimal collagen fibers among apparently normal muscle fibers in subgroup Vb.
[j]: Quantitative histogram of the mean area percentage of collagen fibers deposition across all experimental groups.

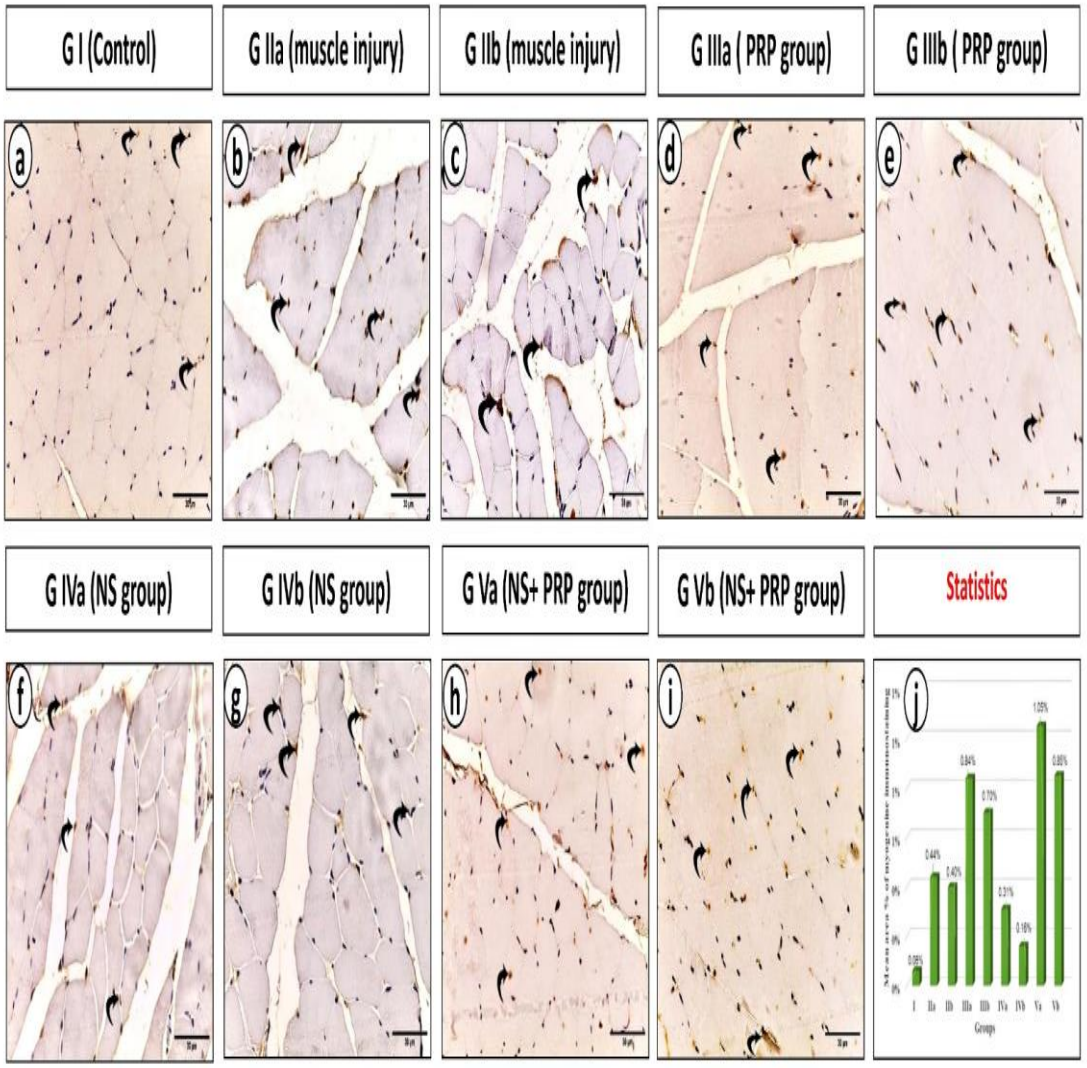

Fig. 3: [**a –i]: Photomicrographs of rat gastrocnemius muscle sections immunostained for myogenin (X400), illustrating the extent of nuclear myogenin immunoreactivity across groups (arrows): [a]:** Very minimal myogenin immunoreaction in control group. **[b]:** Weak myogenin immunoreactivity in subgroup IIa **[c]**: Weak immunreaction in subgroup IIb. **[d]:** Moderate myogenin immunreactivity in subgroup IIIa. **[e]:** Moderate myogenin immunostaining in subgroup IIIb**. [f]:** Weak immunoreaction in subgroup IVa**. [g]:** Weak myogenin immunoreactivity in subgroup IVb. **[h]:** Strong myogenin immunostaining in subgroup Va. **[i]:** strong immunoreactivity in subgroup Vb**.**
[j]: Histogram showing the mean area percentage of Myogenin immunoreactivity in all experimental groups**.**

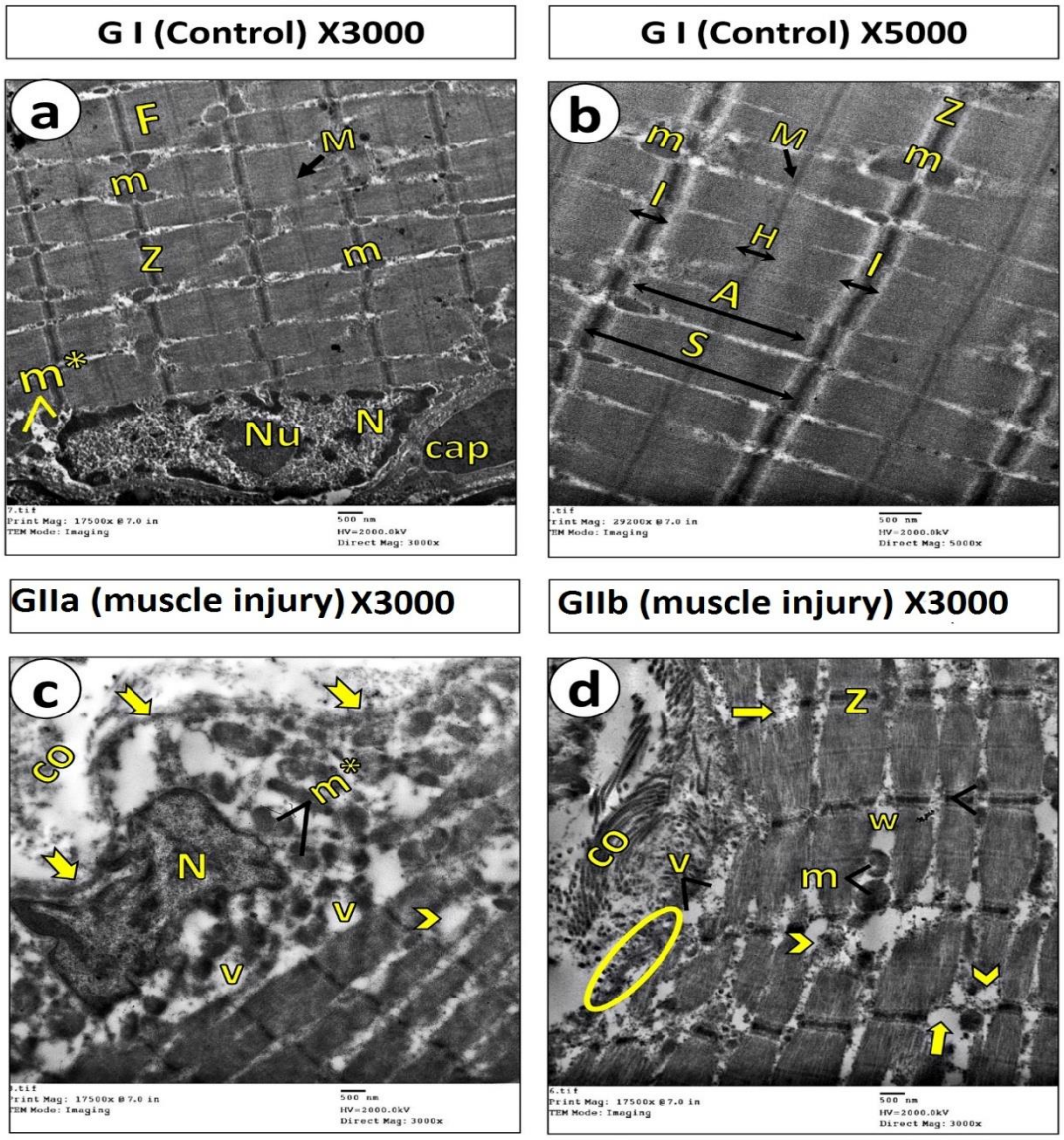

Fig. 4: EM micrographs of rat gastrocnemius muscle ultrathin sections: [a]: shows myofibrils and myofilaments (F) with alternating light (I) and dark (A) bands, Z line (Z). bisecting each I band, M line (M) bisecting each A band, oval euchromatic nucleus (N) with nucleolus (Nu). Small mitochondria (m) present in the sarcoplasm between the myofibrils and as couples at the level of Z line, perinuclear mitochondria (m*) near the nucleus beneath the sarcolemma and blood capillary (cap). [b]: Higher magnifications of the previous section to show the structure of sarcomere. There are alternating light bands (I) and dark bands (A), Dark Z lines bisecting the I bands (Z), M lines (M) bisecting the H bands (H) which appear in the center of dark bands and Mitochondria (m) between myofibrils. The region between two consecutive Z lines constitutes a single sarcomere (S). [c]: Shows irregular myofibrils with degenerated myofilaments (arrow heads), vacuolations (V), abnormal shaped nucleus (N) with irregular chromatin distribution and irregular outline, perinuclear mitochondria (m*) with different sizes and abnormal matrix density and intermyofibrillar mitochondria are not seen, an undulated irregular sarcolemma (arrows) and collagen fibers in the endomysium (CO) [d] Shows degenerated myofilaments (arrow heads) with interruptions of Z lines (thick arrows), vacuolations (V), wide spaces between myofibrils (W) and intermyofibrillar mitochondria which are few and have different sizes (m), loss of integrity of sarcolemma (circle) and collagen fibers (CO) accumulated in the endomysium with some of them are transversely arranged and others are longitudinally arranged denoting irregularity.

G IIIa (PRP group)

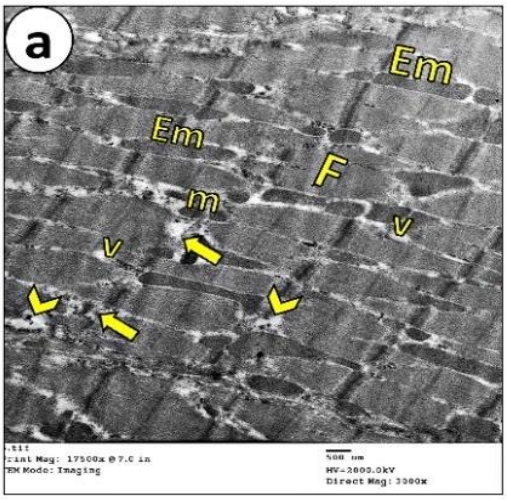

G IIIb (PRP group)

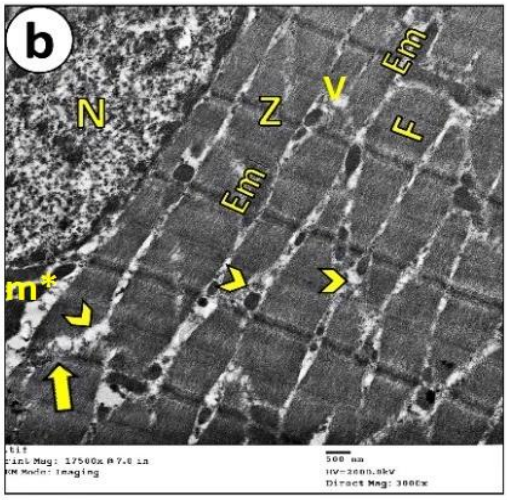

G IVa (NS group)

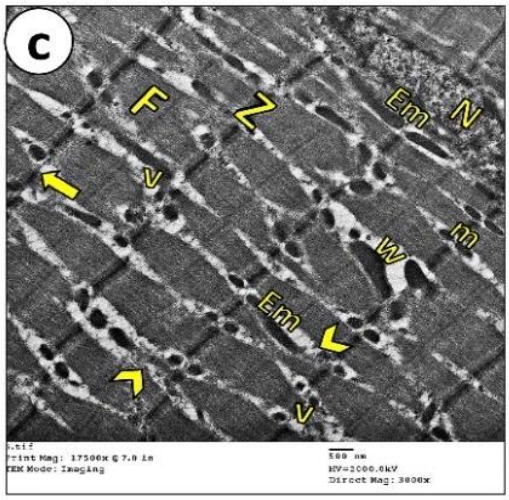

G IVb (NS group)

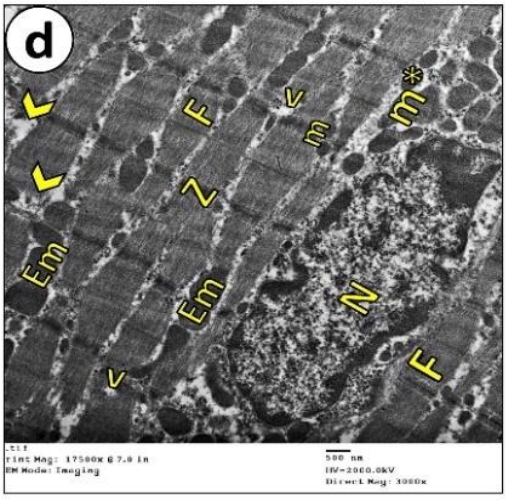

G Va (NS+ PRP group)

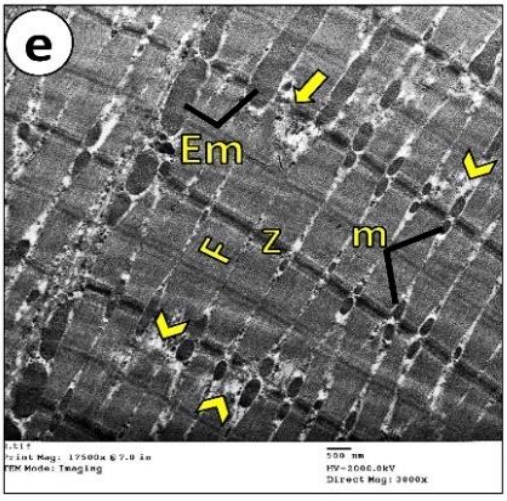

G Vb (NS+ PRP group)

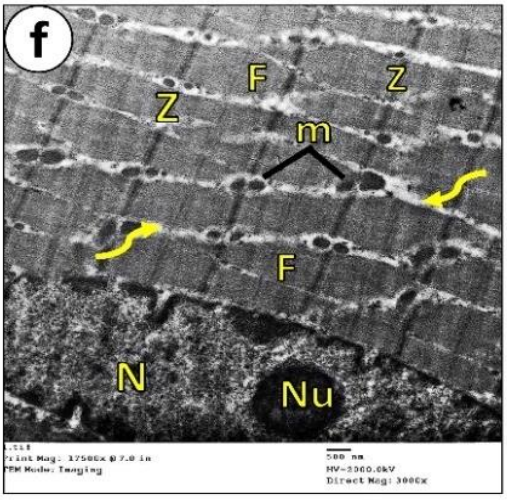

Fig. 5: EM micrographs of rat gastrocnemius muscle ultrathin sections: [a]: Shows myofibrils and myofilaments (F) with alternating dark and light bands, little degenerated myofilaments (arrow heads), some interrupted Z lines (thick arrows), little vacuolations (V), pairs of small rounded mitochondria at Z line (m) and multiple elongated mitochondria (Em). **[b]:** Shows apparently normal myofibrils and myofilaments (F) with well registered Z lines (Z), little degenerated myofilaments (arrow heads), interruptions of Z lines (thick arrows), little vacuolations (V), few elongated mitochondria (Em) , mitochondria at the periphery near the nucleus (m*) and a part of elongated euchromatic nucleus (N) **[c]:** Shows myofibrils and myofilaments (F) with Z lines (Z), elongated and euchromatic.nucleus (N), some degenerated myofilaments (arrow heads), some interruptions of Z lines (thick arrows), some vacuolations (V), little widening of spaces between myofibrils (W), some small rounded and paired mitochondria (m) and many elongated mitochondria (Em) **[d]:** Shows apparently normal myofibrils and myofilaments (F), Z lines (Z) bisecting I bands, euchromatic oval nucleus (N) present between myofibrils (internalized), little degenerated myofilaments (arrow heads), little vacuolations (V), small rounded mitochondria (m) appearing in pairs at Z lines, multiple enlarged mitochondria (Em) with normal structure and matrix density and multiple mitochondria at the periphery near the nucleus (m*) with some are enlarged. **[e]:** Shows apparently normal myofibrils and myofilaments (F) with nearly normal sarcomeric pattern except for few degenerated myofilaments (arrow heads), well aligned Z lines (Z) with only few interrupted Z lines (thick arrow), multiple pairs of small rounded to oval mitochondria at Z line (m) and many enlarged and elongated mitochondria (Em) with normal structure and matrix density. **[f]:** Shows apparently normal myofibrils and myofilaments (F) with almost normal sarcomeric pattern with well registered Z lines (Z), narrow intervening spaces between myofibrils (zigzag arrows) as normal, a prominent nucleolus (Nu) within euchromatic oval nucleus (N) and numerous small mitochondria (m) in pairs at Z lines (microscopic magnification: X 3000).

Table (1): Data represent the mean area percentage ± SD of collagen fiber deposition across Groups I–V; statistical comparisons were conducted using post hoc LSD analysis.

	Group I	Group II		Group III		Group IV		Group V	
		IIa	IIb	IIIa	IIIb	Iva	Ib	Va	Vb
Mean area %	0.38	11.37	11.11	2.72	1.95	5.52	3.56	1.48	0.39
SD±	0.03	0.7954	0.8315	0.2784	0.2026	0.3813	0.3446	0.1730	0.0321
Significance at P < 0.01	2,3,4,5, 6,7,8	1,4,5, 6,7,8,9	1,4,5, 6,7,8,9	1,2,3, 5, 6,7,8,9	1,2,3,4, 6,7,8,9	1,2,3,4, 5,7,8,9	1,2,3,4, 5,6,8,9	1,2,3,4, 5,6,7,9	2,3,4,5, 6,7,8

1=sig. with group I 2=sig. with group IIa 3=sig. with group IIb 4=sig. with group IIIa 5=sig. with group IIIb 6=sig. with group IVa 7=sig. with group IVb 8=sig. with group Va 9=sig. with group Vb

Table (2): Myogenin immunostaining expressed as mean area percentage ± SD across Groups I–V; intergroup comparisons were conducted using post hoc LSD analysis."

	Group I	Group II		Group III		Group IV		Group V	
		IIa	IIb	IIIa	IIIb	Iva	IVb	Va	Vb
Mean area %	0.06	0.44	0.40	0.84	0.70	0.31	0.16	1.05	0.85
SD±	0.0157	0.0302	0.0241	0.0277	0.0180	0.0186	0.0227	0.0443	0.0275
Significance at P < 0.01	2,3,4,5, 6,7,8,9	1,4,5, 6,7,8,9	1,4,5, 6,7,8,9	1,2,3, 5, 6,7,8	1,2,3,4, 6,7,8,9	1,2,3,4, 5,7,8,9	1,2,3,4, 5,6,8,9	1,2,3,4, 5,6,7,9	1,2,3,5, 6,7,8

1=sig. with group I 2=sig. with group IIa 3=sig. with group IIb 4=sig. with group IIIa 5=sig. with group IIIb 6=sig. with group IVa 7=sig. with group IVb 8=sig. with group Va 9=sig. with group Vb

DISCUSSION

Skeletal muscle is essential for posture, movement, and energy metabolism. In athletes, frequent musculoskeletal injuries highlight the importance of muscle regeneration for recovery [1, 22].

In our study, group II showed muscle fiber degeneration. The damage in subgroup IIa (at day 7 after injury) persisted in subgroup IIb (at day 14 after injury) with very little improvement. Compared to group I, Masson's trichrome-stained sections from group II demonstrated a significant upregulation ($P < 0.01$) in collagen and a significant upregulation ($P < 0.01$) of myogenin expression. These findings align with previous studies [23- 27]. Several studies [28–31] have also demonstrated increased myogenin immunoreactivity following muscle injury induced by crush or barium chloride, indicating its role in the regenerative process.

Glycerol causes significant ultrastructural damages as detected in our results. It induces myofiber damage by disrupting the basal lamina, loss of integrity of sarcolemma and activating proteolytic enzymes, causing fiber necrosis [32, 33]. Injury initiates degeneration, inflammation, and regeneration; incomplete repair results in fibrosis [34–36]. Neutrophils infiltrate first, followed by monocytes, which differentiate into macrophages within the muscle [37]. M1 macrophages produce proinflammatory

cytokines and ROS, while M2 macrophages secrete anti-inflammatory cytokines to resolve inflammation [38].

Muscle regeneration comprises SCs activation, proliferation, differentiation, and ECM remodeling [39, 40]. This process is governed by myogenic factors—Myf5, MyoD, Myf4, and myogenin—which control myogenic commitment, proliferation, and fusion into myofibers [41]. Myogenin plays a key role in myoblast differentiation and fusion; its deficiency severely impairs muscle regeneration [42]. Fibro/adipogenic progenitors (FAPs) support activation and differentiation of SCs and share in ECM formation during muscle regeneration but typically undergo apoptosis afterward. However, FAPs can differentiate into adipocytes and myofibroblasts, leading to fibrosis [43, 44].

M1 macrophages enhance the proliferation of SCs, while M2 macrophages induce the differentiation of SCs into myoblasts and their fusion into multinucleated myotubes [45]. An imbalance between M1 and M2 macrophage activation elevates TGF-β, which stimulates fibroblasts, suppresses FAPs apoptosis, and promotes their fibrogenic differentiation, resulting in fibrosis [46].

Skeletal muscles have the capacity to repair minor injuries, but the behavior of SCs is controlled by multiple factors as aging, injury severity, degree of inflammation, state of ECM, affection of basal lamina and dystrophin of cytoskeleton, innervation and vascular supply [3, 45, 47].

Our findings align with previous reports [13, 33, 48, 49], which demonstrated persistent muscle damage, impaired regeneration, and fibrosis 14 days' post-glycerol injury, linked to basal lamina disruption, delayed macrophage differentiation, and FAP accumulation.

Herein, PRP administration in subgroup IIIa reduced the muscle damage and enhanced the regeneration of muscle fibers. The injury was evidently milder compared to group II. Regenerating muscle fibers with internalized myonuclei were observed, with further improvement by day 14 (subgroup IIIb). Group III showed a significant decline in collagen deposition and a marked elevation in myogenin expression compared to groups I and II ($P<0.01$). Our observations align with prior researches [29, 50–53]

demonstrating that PRP enhances muscle repair by reducing fibrosis and increasing myogenin levels.

The observed effects are ascribed to the bioactive molecules secreted from activated platelets, such as PDGFs, IGF-1, and VEGF, cytokines, and platelet lysosomes, which activate SCs migration, proliferation and differentiation [8,31 54-56]. Additionally, platelet-derived factors reduce inflammation, oxidative stress markers and pain [57- 59].

A recent study [60] showed that PRP reduces ROS and promotes mitochondrial biogenesis, protecting against mitochondrial injury. Healthy mitochondria support SCs proliferation, differentiation, and energy production during regeneration. In our study, the PRP group exhibited enlarged mitochondria due to enhanced fusion and biogenesis, boosting the energy capacity of regenerating muscle [61, 62].

Platelet-rich plasma (PRP) promotes angiogenesis via PDGFs and VEGF, enhancing vascularization to support tissue repair [63, 64]. Additionally, PRP inhibits TGFβ1-induced fibroblast-to-myofibroblast transition through VEGF-A, reducing fibrosis [65].

Nigella sativa (NS) administration in Group IV modestly reduced muscle damage and promoted myofiber regeneration. On day 7 post-injury (subgroup IVa), tissue damage was slightly attenuated compared to Group II, while greater regenerative improvement was observed by day 14 (subgroup IVb). In comparison to group II, a statistically significant decline ($P<0.01$) in collagen fiber accumulation was noted in group IV. Relative to group I, a significant elevation ($P<0.01$) in myogenin immunostaining was detected in subgroup IVa. Versus group II, there was some significant decline ($P<0.01$) in myogenin immunostaining in subgroup IVb. These findings align with previous studies [15, 66–68] indicating that NS or its active constituents improve skeletal muscle injury and enhance regeneration.

Many studies showed that NS exhibit anti-inflammatory, antioxidative, hypoglycemic and antineoplastic activities [69-74]. Studies [62, 75] have shown that NS, through its antioxidant and anti-inflammatory properties, preserves mitochondrial integrity, promotes biogenesis and fusion, and supports tissue regeneration. Additionally, dithymoquinone, a bioactive compound in NS, inhibits myostatin, thereby enhancing muscle regeneration [76, 77].

Contrary to our research, one study [78] found no effect of NS on muscle damage or inflammation, likely due to limitations such as NS being in oil form, a short two-week intake, and the injury method, which may have reduced absorption and efficacy.

Combined administration of PRP and NS in group V showed very minimal muscle damage. The improvement was more obvious in subgroup Vb (on day 14 post injury) than subgroup Va (on day 7 post injury). In comparison to group II, a significant decline ($P<0.01$) in collagen area was identified in group V. Relative to group I, an insignificant elevation ($P<0.01$) in collagen fibers deposition in subgroup Vb was observed. A significant increase ($P<0.01$) in myogenin immunostaining was detected in group V when compared to group II.

The combined effects of NS and PRP likely explain these results. Pre-treatment with NS before glycerol injection reduced damage and inflammation, creating conditions favorable for muscle regeneration [68]. Studies also show that administering NS prior to injury is more effective than afterward, owing to its antioxidant and anti-inflammatory actions [66]. Additionally, PRP given afterward further minimized damage and enhanced muscle fiber regeneration and differentiation, likely through its direct trophic effects [53,54].

CONCLUSION

Histological and ultrastructural analyses showed that glycerol produced significant myofiber damage, inflammation, and delayed regeneration with excessive collagen deposition. PRP significantly reduced injury, increased myogenin expression, enhanced muscle regeneration and decreased fibrosis. NS showed moderate regenerative effects. Combined administration of PRP and NS effectively mitigated glycerol-induced muscle injury, reduced fibrosis and enhanced myogenic differentiation suggesting a synergistic effect of the two treatments.

Limitations

Although our results were promising, future studies could build on this work in several ways. This study was limited to male albino rats, restricting the evaluation of potential sex-related differences, and did not include functional or biochemical assessments to comprehensively assess muscle recovery.

Recommendations

Subsequent research should involve subjects of both sexes, to assess sex-related differences in muscle regeneration and extend observation periods. Combining functional, biochemical, and histological assessments would offer a more comprehensive view of muscle recovery. Additionally, exploring different doses and formulations of NS and PRP could help optimize their effects on muscle repair.

Funding

This research received no financial support.

Author contribution

Each author participated equally in the completion of this work

NO conflicts of interest

REFERENCES

1. Sicherer ST, Venkatarama RS, Grasman JM. Recent Trends in injury models to study skeletal muscle regeneration and repair. Bioengineering 2020; 7 (76): 1-11. DOI: 10.3390/bioengineering7030076.

2. Mahdy MAA. Glycerol-induced injury as a new model of muscle regeneration. Cell Tissue Res 2018; 374: 233–241. DOI: 10.1007/s00441-018-2846-6.

3. Anderson JE. Key concepts in muscle regeneration: muscle "cellular ecology" integrates a gestalt of cellular cross-talk, motility, and activity to remodel structure and restore function. European J of Applied Physiology 2021; 122 (2): 273-300. DOI: 10.1007/s00421-021-04865-4.

4. Morgan JE, Partridge TA. Muscle satellite cells. Int J Biochem Cell Biol 2003; 35 (8): 1151-1156. DOI: 10.1016/S1357-2725(03)00042-6.

5. Chen W, Datzkiw D, Rudnicki MA. Satellite cells in ageing: use it or lose it. Open Biol 2020; 10: 200048. DOI: 10.1098/rsob.200048.

6. Popescu MN, Iliescu MG, Beiu C, Popa LG, Mihai MM, Berteanu M, et al. Autologous Platelet-Rich Plasma Efficacy in the Field of Regenerative Medicine:

Product and Quality Control. Bio Med Research International 2021; Volume 2021, Article ID 4672959, 6 pages. DOI: 10.1155/2021/4672959.

7. Everts P, Onishi K, Jayaram P, Lana JF, Mautner, K. Platelet-Rich Plasma: New Performance Understandings and Therapeutic Considerations in 2020. Int J Mol Sci 2020; 21: 7794, 36 pages. DOI: 10.3390/ijms21207794.

8. Rodriguez AE, Gisbert S, Palazon A, Alio JL. Quantification of growth factors and fibronectin in diverse preparations of platelet-rich plasma for the treatment of ocular surface disorders (E-PRP). Trans Vis Sci Tech 2020; 9 (6): 22, 10 pages. DOI: 10.1167/tvst.9.6.22.

9. Tsai WC, Yu TY, Lin LP, Lin MS, Wu YC, Liao CH, et al. Platelet rich plasma releasate promotes proliferation of skeletal muscle cells in association with upregulation of PCNA, cyclins and cyclin dependent kinases. Platelets 2017; 28: 491 - 497. DOI: 10.1080/09537104.2016.1227061.

10. Ijaz H, Tulain UR, Qureshi J, Danish Z, Musayab S, Akhtar MF, et al. Nigella sativa (Prophetic Medicine): A Review. Pak J Pharm Sci 2017; 30 (1): 229–234. PMID**:** 28603137**.**

11. Areefa A, Mohd A, Shah, CS. A Review on Nigella sativa (Kalonji) Seeds: A Universal Healer Cell Med 2020; 10 (2): e11. DOI: 10.5667/CellMed.2020.0011.

12. Hannan MA, Rahman MA, Sohag AAM, Uddin MJ, Dash R, Sikder MH, et al. Black Cumin (Nigella sativa L.): A Comprehensive Review on Phytochemistry, Health Benefits, Molecular Pharmacology and Safety. Nutrients 2021; 13: 1784. DOI: 10.3390/nu13061784.

13. Mahdy MAA, Warita K, Hosak YZ. Neutralization of transforming growth factor (TGF)-β1 activity reduced fibrosis and enhanced regeneration of glycerol-injured rat muscle. J Vet Med Sci 2020; 82 (2): 168–171. DOI: 10.1292/jvms.19-0446.

14. Attia GM, Atef H, Elmansy RA. Autologous platelet rich plasma enhances satellite cells expression of MyoD and exerts angiogenic and antifibrotic effects in experimental rat model of traumatic skeletal muscle injury. EJH 2017; 40 (4): 443-458. DOI: 10.21608/EJH.2018.5513.

15. Rahman M, Yang DY, Kim GB, Lee SJ, Kim, SJ. Nigella sativa seed extract attenuates the fatigue induced by exhaustive swimming in rats. Biomedical Reports 2017; 6 (4): 468-474. DOI: 10.3892/br.2017.866.

16. Al-Saffar RAS, Al-Wiswasy MKM. A Morphological Study of the Pharmacological Effects of the Nigella sativa on the Reproductive System in Experimental Rats. Jordan Journal of Biological Sciences 2019; 12 (2): 147 – 153. ISSN 1995-6673.

17. Contreras-Mun˜oz P, Torrella JR, Serres X, Rizo-Roca D, De la Varga M, Viscor G, et al. Postinjury Exercise and Platelet-Rich Plasma Therapies Improve Skeletal Muscle Healing in Rats But Are Not Synergistic When Combined. AJSM 2017; 20 (10): 1-11. DOI: 10.1177/0363546517702864.

18. Nada FF, El-Safty FEA, El –mehi AE, Issa NM. The Possible Protective Effect of Platelet Rich Plasma on Aspirin Induced Gastric Ulcer in Adult Male Albino Rat. The Egyptian Journal of Hospital Medicine 2020; 81 (1): 1240-1250. Doi: 10.21608/ejhm.2020.112312.

19. Bancroft JD, Layton C. The Haematoxyline and Eosin and Connective and other mesenchymal tissues with their stains. In: Bancroft's Theory & Practice of Histological Techniques. Eds. Suvarna, S. K.; Layton, C. and Bancroft, J. D. 8th ed., Ch. 10 & 12, Churchill Livingstone of El Sevier, Philadelphia, 2019; PP 126-139 and 153-175.

20. Sanderson T, Wild G, Cull AM, Marston J, Zardin G. Immunohistochemical and immunofluorescent techniques. In: Bancroft's Theory & Practice of Histological Techniques. Eds. Suvarna, S. K.; Layton, C. and Bancroft, J. D. 8th ed., Ch. 19, Churchill Livingstone of El Sevier, Philadelphia, 2019; PP 337- 394.

21. Woods JD, Stirling JW. Transmission electron microscopy. In: Bancroft's Theory & Practice of Histological Techniques. Eds. Suvarna, S. K.; Layton, C. and Bancroft, J. D. 8th ed., Ch. 21, Churchill Livingstone of El Sevier, Philadelphia, 2019; PP 434-475.

22. Giudice J, Taylor JM. Muscle as a paracrine and endocrine organ. Curr Opin Pharmacol 2017; 34: 49-55. DOI: 10.1016/j.coph.2017.05.005.

23. Mahdy MAA, Lei HY, Wakamatsu J-I, Hosak YZ, Nishimura T. Comparative study of muscle regeneration following cardiotoxin and glycerol injury. Ann Anat 2015; 202: 18–27. DOI: 10.1016/j.aanat.2015.07.002.

24. Rigon M, Horner SJ, Straka T, Bieback K, Gretz, N, Hafner M, et al. "Effects of ASC application on NMJ regeneration upon glycerol-induced muscle damage". Front Mol Neurosc 2020; 13 (107): 13 pages. DOI: 10.3389/fnmol.2020.00107.

25. Mahdy MAA, Akl MA, Madkour FA. Effect of chitosan and curcumin nanoparticles against skeletal muscle fibrosis at early regenerative stage of glycerol -injured rat muscles. BMC Musculoskeletal Disorders 2022; 23: 670. 13 pages. DOI. 10.1186/s12891-022-05633-x.

26. Noonan AM, Buliung E, Josh Briar K, Quinonez D, Séguin CA, Brown SHM. Glycerol induced paraspinal muscle degeneration leads to hyper-kyphotic spinal deformity in wild-type mice. Scientific Reports 2023; 13 (8170), 15 pages. DOI: 10.1038/s41598-023-35506-9.

27. Su CM, Tsai CH, Chen HT, Wu YS, Chang JW, Yang SF, et al. Melatonin improves muscle injury and differentiation by increasing Pax7 expression. int J Biol Sci 2023; 19 (4): 1049-1062. DOI: 10.7150/ijbs.79169.

28. Mehanna RA, Soliman GY, Hassaan, PS, Sharara, GM, Abdel Monei, RA. Protective role of melatonin on skeletal muscle injury in rats. Int J Clin Exp Med 2017; 10 (1): 1490-1501.DOI: 10.3885/ijcem0038460.

29. Ahmed AM, Abo Elfadl SG, Ismail DS, Filobbos SA. Histological Study on the Possible Role of Platelet Rich Plasma in Repair of induced Acute Skeletal Muscle Injury in Adult Male Albino Rats. EJH 2024; 47 (2): 632- 645. DOI: 0.21608/ejh.2023.199071.1870

30. Srikuea R, Hirunsai M. Effects of intramuscular administration of 1, 25 (OH) 2D3 during skeletal muscle regeneration on regenerative capacity, muscular fibrosis and

angiogenesis. J Appl Physiol 2016; 120 (12): 1381–1393. DOI: 10.1152/japplphysiol.01018.2015.

31. Cianforlini M, Grassi M, Coppa V, Manzotti S, Orlando F, Mattoli-Belmonte M, et al. Skeletal muscle repair in a rat muscle injury model: the role of growth hormone (GH) injection. European Review for Medical and Pharmacological Sciences 2020; 24: 8566-8572. DOI: 10.26355/eurrev_202008_22652.

32. Demonbreun AR, Rossi, AE, Alvarez MG, Swanson KE, Deveaux HK, Earley JU, et al. Dysferlin and myoferlin regulate transverse tubule formation and glycerol sensitivity. Am J Pathol 2014; 184 (1): 248–259. DOI: 10.1016/j.ajpath.2013.09.009.

33. Mahdy MAA, Warita K, and Hosaka YZ. Early ultrastructural events of skeletal muscle damage following cardiotoxin-induced injury and glycerol-induced injury. Micron 2016; 91: 29–40. DOI: 10.1016/j.micron.2016.09.009.

34. Ten Broek RW, Grefte S; Von den Hoff JW. Regulatory factors and cell populations involved in skeletal muscle regeneration. Journal of cellular physiology 2010; 224 (1): 7–16. DOI: 10.1002/jcp.22127.

35. Mackey AL, Kjaer M. The breaking and making of healthy adult human skeletal muscle in vivo. Skelet Muscle 2017; 7: 24, 18 pages. DOI: 10.1186/ s13395-017-0142-x.

36. Mehanna MS, Abdallah EA, Al-Shahed FAN, Al-Azab HW. Effect of Simvastatin on the Skeletal Muscles of Senile Male Albino Rats and Possible Protective Role of L-Carnitine. A Histological Study. EJH 2020; 43, (1): 286-300. DOI: 10.21608/ejh.2019.17989.1184.

37. Uderhardt S, Martins A J, Tsang J S, Lämmermann T, Germain RN. Resident macrophages cloak tissue microlesions to prevent neutrophil-driven inflammatory damage. Cell 2019; 177: 541–555. e517. DOI: 10.1016/j. cell.2019.02.028.

38. Pérez S, Rius-Pérez S. Macrophage Polarization and Reprogramming in Acute Inflammation: A Redox Perspective. Antioxidants 2022; 11, 1394, 23 pages. DOI: 10.3390/antiox 11071394.

39. Laumonier T, Menetrey J. Muscle injuries and strategies for improving their repair. J Exp Orthop 2016; 3: 1–9. DOI: 10.1186/s40634-016-0051-7.

40. Marwan TM Abofila, Azab E Azab, Asma N Bshena. Skeletal Muscles: Insight into Embryonic Development, Satellite Cells, Histology, Ultrastructure, Innervation, Contraction and Relaxation, Causes, Pathophysiology, and Treatment of Volumetric Muscle Injury. J Biotech and Bioprocessing 2021; 2 (4). DOI: 10.31579/2766-2314/0.

41. Esteves de Lima J, Relaix F. Master regulators of skeletal muscle lineage development and pluripotent stem cells differentiation. Cell Regener (London, England) 2021; 10: 31. DOI: 10.1186/s13619-021-00093-5.

42. Benavente-Diaz M, Comai G, Di Girolamo D, Langa F, Tajbakhsh S. Dynamics of myogenic differentiation using a novel Myogenin knock-in reporter mouse. Skeletal Muscle 2021; 11 (5): 13 pages. DOI: 10.1186/s13395-021-00260-x.

43. Giuliani G, Rosin M, Reggio A. Signaling pathways regulating the fate of fibro/adipogenic progenitors (FAPs) in skeletal muscle regeneration and disease. FEBSJ 2021; 289: 6484-6517. DOI:10.1111/febs.16080.

44. Kaur G, Davies MR, Liu X, Feeley BT. The Role of Fibro-Adipogenic Progenitors in Musculoskeletal Disease. Muscles, Ligaments and Tendons Journal 2021; 11 (2): 201-214. DOI: 10.32098/mltj.02.2021.01.

45. Chazaud B. Inflammation and skeletal muscle regeneration: leave it to the macrophages! Trends Immunol 2020; 41: 481–492. DOI: 10.1016/j.it.2020.04.006.

46. Perandini LA, Chimin P, Lutkemeyer DDS, Camara NOS. Chronic inflammation in skeletal muscle impairs satellite cells function during regeneration: can physical exercise restore the satellite cell niche? FEBSJ 2018; 285 (11): 1973-198. DOI: 10.1111/febs.14417.

47. Kok HJ, Barton ER. Actions and interactions of IGF-I and MMPs during muscle regeneration. Semin Cell Dev Biol 2021; 119: 11–22. DOI: 10.1016/j.semcdb.2021.04.018.

48. Munoz-Canoves P, Serrano AL. Macrophages decide between regeneration and fibrosis in muscle. Trends Endocrinol Metab 2015; 26: 449–450. DOI:10.1016/j.tem.2015.07.005.

49. Yao L, Tichy ED, Zhong L, Mohanty S, Wang L, Ai E, et al. Gli1 defines a subset of fibro-adipogenic progenitors that promote skeletal muscle regeneration with less fat accumulation. J Bone Miner Res 2021; 36:1159–1173. DOI: 10.1002/jbmr.4265.

50. Dzhyvak V, Klishch I, Datsko T, Khlibovska O. Influence of PRP on morphological changes in muscle in the early period after traumatic muscle injury in the experiment. Journal of Education, Health and Sport 2020; 10 (6): 171-178. DOI: 10.12775/JEHS.2020.10.06.019.

51. Elkaliny HH, El-Abd SS, Ibrahim, MAA. Platelet-rich Plasma Enhances Recovery of Skeletal Muscle Atrophy after Immobilization Stress in Rat: A Histological and Immunohistochemical Study. EJH 2020; 44 (3): 719-731. DOI: 10.21608/ejh.2020.44196.1363.

52. Rtail R, Maksymova O, Illiashenko V, Gortynska O, Korenkov O, Moskalenko P, et al. Improvement of Skeletal Muscle Regeneration by Platelet-Rich Plasma in Rats with Experimental Chronic Hyperglycemia. Bio Med Research International 2020. Article ID 6980607, 9 pages. DOI: 10.1155/2020/6980607.

53. Gao H, Zhao Z, Li J, Guo Z, Zhang F, Wang K, et al. Platelet-rich plasma promotes skeletal muscle regeneration and neuromuscular functional reconstitution in a concentration dependent manner in a rat laceration model. Biochemical and Biophysical Research Communications 2023; 672: 185-192. DOI: j.bbrc.2023.05.123.

54. Qian Y, Han Q, Chen W, Song J, Zhao X, Ouyang Y, et al. Platelet-rich plasma derived growth factors contribute to stem cell differentiation in musculoskeletal regeneration. Front Chem 2017; 5: 89. DOI: 10.3389/fchem.2017. 00089.

55. Eisinger F, Patzelt J, Langer HF. The platelet response to tissue injury. Frontiers in Medicine 2018; 5: 317. DOI: 10.3389/fmed.2018.00317.

56. Duan C, Ren H, Gao S. Insulin-like growth factors (IGFs), IGF receptors, and IGF-binding proteins: Roles in skeletal muscle growth and differentiation. Gen Comp Endocrinol 2010; 167: 344-351. DOI: 10.1016/j.ygcen.2010.04.009.

57. Tao ZY, Wang PX, Wei SQ, Traub RJ, Li JF, Cao, DY. The Role of Descending Pain Modulation in Chronic Primary Pain: Potential Application of Drugs Targeting Serotonergic System. Neural Plast 2019; 2019: 1389296. DOI: 10.1155/2019/1389296.

58. Lai L, Mohamed MNA, Ali MRM, Teng-Keen K Yusof A. Effect of Platelet-Rich Plasma Treatment on Antioxidant Enzymes Activity following Hamstring Injury among Malaysian Athletes. Sains Malaysiana 2016; 45 (5): 769–775. DOI: 10.17576/jsm-2016-4505-06.

59. Hegab II, Abd-Ellatif RN, Atef MM. Effect of Platelet Rich Plasma on an Experimental Rat Model of Adriamycin Induced Chronic Kidney Disease. Med J Cairo Univ 2019; 87(3): 2207-2217. DOI: 10.21608/MJCU.2019.54382.

60. Li M, Han H, Chen L, Li H. Platelet-rich plasma contributes to chondroprotection by repairing mitochondrial function via AMPK/NF-κB signaling in osteoarthritic chondrocytes. Tissue Cell 2022; 77: 101830. DOI: 10.1016/j.tice.2022.101830.

61. Rahman FA, Quadrilatero J. Mitochondrial network remodeling: An important feature of myogenesis and skeletal muscle regeneration. Cell Mol Life Sci 2021; 78: 4653–4675. DOI: 10.1007/s00018-021-03807-9.

62. Alway SE, Paez HG, Pitzer CR. The Role of Mitochondria in Mediation of Skeletal Muscle Repair. Muscles 2023; 2: 119–163. DOI: 10.3390/ muscles2020011.

63. Martínez CE, Smith PC, Palma Alvarado VA. The influence of platelet-derived products on angiogenesis and tissue repair: a concise update. Front Physiol 2015; 6: 290. DOI: 10.3389/fphys.2015.00290.

64. Marushima A, Nieminen M, Kremenetskaia I, Gianni-Barrera R, Woitzik J, von Degenfeld G, et al. Balanced single-vector co-delivery of VEGF/PDGF-BB improves functional collateralization in chronic cerebral ischemia. J Cereb Blood Flow Metab 2020; 40: 404–419. DOI: 10.1177/0271678X18818298.

65. Chellini F, Tani A, Nosi D, Pavan P, Orlandini SZ, Sassoli C. Platelet-Rich Plasma Prevents In Vitro Transforming Growth Factor-1- Induced Fibroblast to Myofibroblast Transition: Involvement of Vascular Endothelial Growth Factor (VEGF)-A/VEGF Receptor-1-Mediated Signaling. Cells 2018; 7: 142, 21 pages. DOI: 10.3390/cells7090142.

66. Elsawy SGS, Kamal KAE, Zouair MGA. Efficacy OF Thymoquinone In Chemoprevention And Treatment Of Acrylamide-Induced Striated Muscle Degneration Of Rat`s Tongue (Histological And Histochemical Study). AJDS 2019; 22 (1): 1-13. ISSN Portal 1110-2624.

67. Azırak S, Taştemir Korkmaz D, Bilgiç S, Sevimli M, Özer MK. The musculoprotective effects of thymoquinone on ameliorating soleusmuscle damage induced by valproic acid in rats. ADYÜ Sağlık Bilimleri Derg. 2022; 8 (3):170-180. DOI: 10.30569.adiyamansaglik.1202066.

68. Swidan SA, El Azabb SA, Hassan MMA. Effect of Thymoquinone on skeletal muscle regeneration via assessment of Pax-7 and Myo-D expression in the DMBA-treated hamster pouch. Braz Dent Sci 2023; 26 (2): e3620. DOI: 10.4322/bds.2023.e3620.

69. Dalli M, Bekkouch O, Azizi S-e, Azghar A, Gseyra N, Kim B. Nigella sativa L. Phytochemistry and Pharmacological Activities: A Review (2019–2021). Biomolecules 2022; 12: 20. DOI: 10.3390/biom12010020.

70. Pandey R, Pandey B, Bhargava A. An updated review on the phytochemistry and pharmacological activity of black cumin (Nigella sativa L.). Adv Chin Med 2025; 2: 13–29. DOI: 10.1002/acm4.33.

71. Alkis H, Demir E, Taysi MR, Sagir S, Taysi S. Effects of Nigella sativa oil and thymoquinone on radiation-induced oxidative stress in kidney tissue of rats. Biomed Pharmacother 2021; 139: 111540. DOI: 10.1016/j.biopha.2021.111540.

72. Mahmoud HS, Almallah AA, EL-Hak HNG, Aldayel TS, Abdelrazek HMA, Khaled HE. The effect of dietary supplementation with Nigella sativa (black seeds)

mediates immunological function in male Wistar rats. Sci Rep 2021; 11: 7542. DOI: 10.1038/s41598-021-86721-1.

73. Hakim AS, Abouelhag HA, Abdou AM, Fouad EA, Khalaf DD. Assessment of Immunomodulatory Effects of Black Cumin Seed (Nigella sativa) Extract on Macrophage Activity in Vitro. Int J Vet Sci 2019; 8 (4): 385-389. P-ISSN: 2304-3075; E-ISSN 2305-4360.

74. Liang Q, Dong J, Wang S, Shao W, Ahmed AF, Zhang Y, et al. Immunomodulatory effects of Nigella sativa seed polysaccharides by gut microbial and proteomic technologies. Int J Biol Macromol 2021; 184: 483-496. DOI: 10.1016/j.ijbiomac.2021.06.118.

75. Khalifa AA, Rashad RM, El-Hadidy WF. Thymoquinone protects against cardiac mitochondrial DNA loss, oxidative stress, inflammation and apoptosis in isoproterenol-induced myocardial infarction in rats. Heliyon 2021; 7 (7): e07561. DOI: 10.1016/j.heliyon.2021.e07561.

76. Iskenderian A, Liu N, Deng Q, Huang Y, Shen C, Palmieri K, et al. Myostatin and activin blockade by engineered follistatin results in hypertrophy and improves dystrophic pathology in mdx mouse more than myostatin blockade alone. Skelet. Muscle 2018; 8: 34, 16 pages. DOI: 10.1186/s13395-018-0180-z.

77. Ahmad SS, Ahmad K, Lee EJ, Shaikh S, Choi I. Computational Identification of Dithymoquinone as a Potential Inhibitor of Myostatin and Regulator of Muscle Mass. Molecules 2021; 26: 5407, 12 pages. DOI: 10.3390/ molecules26175407.

78. Raimi F, Jawis NM, Zainuddin ZA. Multiple intakee of Nigella Sativa before and after exercise-induced muscle damage does not influence muscle damage and inflammatory cytokines. Journal of Positive School Psychology 2022; 6 (2): 1129 – 1140. ISSN 2717-7564.